**Temperature-related $N_2O$ emission and emission potential of freshwater sediment**

Shuai Li [1,+], Ang Yue [2, 3,+], Selina Sterup Moore [4], Fei Ye [1], Jiapeng Wu [1], Yiguo Hong [1] and Yu Wang[1,*]

1 Key Laboratory for Water Quality and Conservation of the Pearl River Delta, Ministry of Education, Institute of Environmental Research at Greater Bay, Guangzhou University, Guangzhou 510006, China; email: 983773940@qq.com (S.L.); yefei09007@gzhu.edu.cn (F.Y.); wujiapeng@gzhu.edu.cn (J.W.); yghong@gzhu.edu.cn (Y.H.)

2 School of Environmental Science and Engineering, Tianjin University, Tianjin, 300350, China; 576252175@qq.com(A.Y.)

3 Tianjin Eco-Environmental Monitoring Center, Tianjin, 300191, China;

4 Department of Agronomy, Food, Natural Resources, Animals and Environment (DAFNAE), University of Padova, 35122 Padova, Italy; selina.moore@unipd.it (S.S.M.)[*] Correspondence: wangyu@gzhu.edu.cn (Y.W.)

[+] These authors contributed equally to this work.

## 1. DNA Extraction, Sequencing, and Quantitative PCR

Total genomic DNA was extracted from sediment/soil samples (approximately 0.5g) using the FastDNA SPIN Kit for Soil (MP Biomedicals, Califonia, USA) following the manufacturer's instructions. The concentration of extracted DNA was measured with a NanoDrop Lite (Thermo Fisher Scientific, Wilmington, DE, USA), and the DNA quality was examined by 1% (wt./vol) agarose gel electrophoresis. The abundance of *nir* gene (*nirS* and *nirK*) and *nosZ* gene (*nosZ* I and *nosZ* II) in sediments/soil samples were quantified by a LightCycler ® R480 II Real-Time PCR (Roche, Basel, Switzerland). Refer to the Table S1 for specific primer sequence information [55-58]. qPCR results with high amplification efficiency (90–110%) and correlation coefficient values of the standard curve ($r^2$>0.97) were integrated into the analysis.

**Table S1.** Primer pairs used in this study and correspondent qPCR protocols

| Genes | Primers | Primer sequences (5' to 3') | Segment length | Reaction conditions | References |
|---|---|---|---|---|---|
| *nirS* | cd3aF | GTSAACGTSAAGGARACSGG | 426 | 95℃ for 10 min, 40 ×, (95℃ for 15 s, 56℃ for 45 s, 72℃ for 45 s) | [55] |
| | R3cd | GASTTCGGRTGSGTCTTGA | | | |
| *nirK* | Flacu | ATCATGGTSCTGCCGCG | 473 | 95℃ for 2 min, 36 ×, (95℃ for 30 s, 56℃ for 45 s, 72℃ for 45 s) | [56] |
| | R3cu | TTGGTGTTRGACTAGCTCCG | | | |
| *nosZ* I | *nosZ*2F | CGCRACGGCAASAAGGTSMSSGT | 267 | 95℃ for 5 min, 40 ×, (95℃ for 30 s, 68℃ for 1 min, 72℃ for 1 min) | [57] |
| | *nosZ*2R | AKRTGCAKSGCRTGGCAGAA | | | |
| *nosZ* II | nosZ F | CTIGGICCIYTKCAYAC | 746 | 95℃ for 2 min, 40 ×, (95℃ for 15 s, 60℃ for 1 min, 72℃ for 1 min) | [58] |
| | nosZ R | GCIGARCARAAITCBGTRC | | | |

## 2. Results

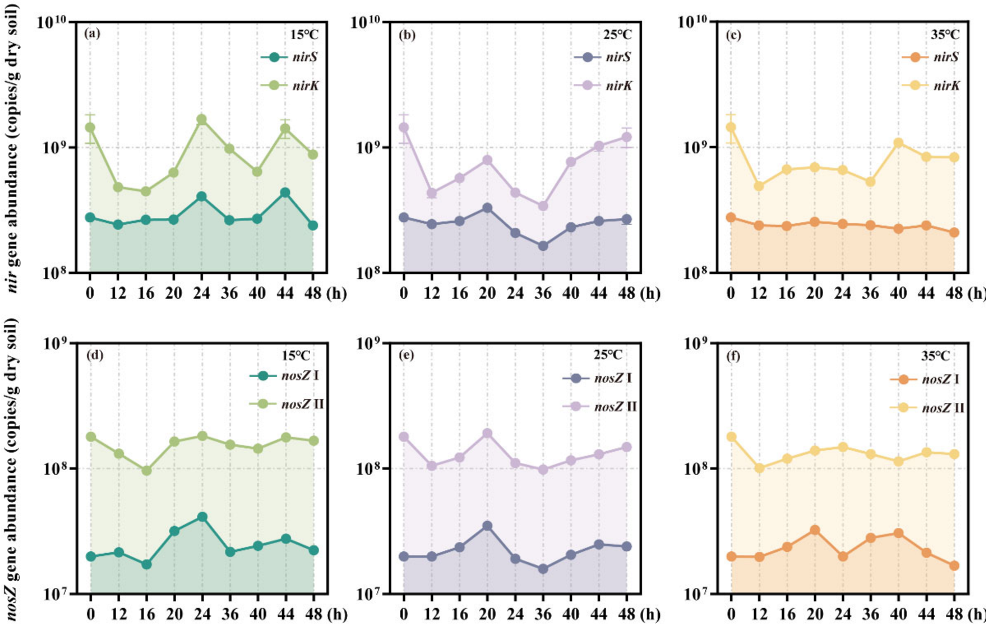


**Figure S1.** The variation of $N_2O$-related functional genes abundance over time.

| Temperature | | p value | | | | | | | | |
|---|---|---|---|---|---|---|---|---|---|---|
| | | $NO_3^-$ | $NO_2^-$ | $NH_4^+$ | DIN | $NO_3^-$/DIN | $NO_2^-$/DIN | $NH_4^+$/DIN | *nirS* / *nirK* | *nosZ* Ⅰ / *nosZ* Ⅱ |
| 15℃ | $D_{N_2O}$ | 0.032 | | | 0.047 | | | 0.026 | | 0.038 |
| | $D_{N_2O}$ / $D_{N_2O}$ + $H_{N_2O}$ | 0.035 | 0.049 | | | | | | | |
| | $H_{N_2O}$ / $D_{N_2O}$ | 0.048 | | | | | | | | |
| 25℃ | $D_{N_2O}$ | | | | | | | | 0.016 | 0.044 |
| | $D_{N_2O}$ + $H_{N_2O}$ | | | | | | | | 0.024 | 0.039 |
| | $D_{N_2O}$ / $D_{N_2O}$ + $H_{N_2O}$ | | | 0.044 | | 0.028 | | 0.028 | 0.02 | |
| | $H_{N_2O}$ / $D_{N_2O}$ + $H_{N_2O}$ | | | | | | | | 0.019 | |
| | $H_{N_2O}$ / $D_{N_2O}$ | | | | | | | | 0.16 | 0.044 |
| 35℃ | $H_{N_2O}$ | 0.019 | 0.008 | | 0.028 | 0 | 0.013 | | | |
| | $D_{N_2O}$ + $H_{N_2O}$ | 0.017 | 0.01 | | 0.026 | 0 | 0.015 | 0.047 | | |
| | $D_{N_2O}$ / $D_{N_2O}$ + $H_{N_2O}$ | 0.017 | 0.01 | | | 0 | 0.015 | 0.047 | | |
| | $H_{N_2O}$ / $D_{N_2O}$ + $H_{N_2O}$ | | 0.001 | | | 0.001 | 0.007 | | | |
| | $H_{N_2O}$ / $D_{N_2O}$ | 0.037 | 0.005 | | 0.043 | 0 | 0.007 | | | |

**Figure S2.** The heatmap of Pearson's correlation coefficients.

The background color of the temperature represented the variation of temperature from light yellow to dark yellow. The shade of the background color represented the size of the value from blue to red.

**Table S2.** The estimated $N_2O$ exchange flux at three different temperatures.

| | 0h | 12h | 16h | 20h | 24h | 36h | 40h | 44h | 48h |
|---|---|---|---|---|---|---|---|---|---|
| Estimated $N_2O$ exchange flux at 15 °C (nmol/m$^2$·h) | 5.03 | 27.19 | 24.92 | 26.47 | 26.75 | 20.84 | 18.83 | 18.39 | 13.83 |
| Estimated $N_2O$ exchange flux at 25 °C (nmol/m$^2$·h) | 5.03 | 59.75 | 55.75 | 60.43 | 47.96 | 27.36 | 23.59 | 19.73 | 16.03 |
| Estimated $N_2O$ exchange flux at 35 °C (nmol/m$^2$·h) | 5.03 | 15.75 | 14.60 | 14.82 | 13.66 | 14.62 | 15.18 | 15.24 | 15.09 |

**Table S3.** Pearson's correlation coefficients between $NO_3^-$, $NO_2^-$, $NH_4^+$, DIN, $NO_3^-$/DIN, $NO_2^-$/DIN, $NH_4^+$/DIN, *nirS*/*nirK*, *nosZ* I /*nosZ* II and $D_{N_2O}$ (dissolved $N_2O$ in overlying water), $E_{N_2O}$ ($N_2O$ emission), $D_{N_2O}+E_{N_2O}$, $D_{N_2O}$/ $D_{N_2O}+E_{N_2O}$, $E_{N_2O}$/ $D_{N_2O}+E_{N_2O}$, $E_{N_2O}$/ $D_{N_2O}$. (*: $p < 0.05$; **: $p < 0.01$; ***: $p < 0.001$)

| | | **Level of significance** | | | | | | | | |
|---|---|---|---|---|---|---|---|---|---|---|
| | | **$NO_3^-$** | **$NO_2^-$** | **$NH_4^+$** | **DIN** | **$NO_3^-$/ DIN** | **$NO_2^-$/DIN** | **$NH_4^+$/DIN** | ***nirS*/*nirK*** | ***nosZ* I/*nosZ* II** |
| | $D_{N_2O}$ | * | | | * | | | * | | * |
| **15°C** | $D_{N_2O}$/ $D_{N_2O}+E_{N_2O}$ | * | * | | | | | | | |
| | $E_{N_2O}$/ $D_{N_2O}$ | * | | | | | | | | |
| | $D_{N_2O}$ | | | | | | | | ** | * |
| | $D_{N_2O}+E_{N_2O}$ | | | | | | | | * | * |
| **25°C** | $D_{N_2O}$/ $D_{N_2O}+E_{N_2O}$ | | | * | | * | | * | * | |
| | $E_{N_2O}$/ $D_{N_2O}+E_{N_2O}$ | | | | | | | | * | |
| | $E_{N_2O}$/ $D_{N_2O}$ | | | | | | | | * | * |
| | $E_{N_2O}$ | * | ** | | * | *** | * | | | |
| | $D_{N_2O}+E_{N_2O}$ | * | ** | | * | *** | * | * | | |
| **35°C** | $D_{N_2O}$/ $D_{N_2O}+E_{N_2O}$ | * | ** | | | *** | * | * | | |
| | $E_{N_2O}$/ $D_{N_2O}+E_{N_2O}$ | | ** | | | ** | ** | | | |
| | $E_{N_2O}$/ $D_{N_2O}$ | | ** | | * | *** | ** | | | |

## References


55. Yergeau, E.; Kang, S.; He, Z.; Zhou, J.; Kowalchuk, G.A. Functional microarray analysis of nitrogen and carbon cycling genes across an Antarctic latitudinal transect. *ISME J.* **2007**, *1*, 163-179.
56. Hallin, S.; Lindgren, P.-E. PCR detection of genes encoding nitrite reductase in denitrifying bacteria. *Appl. Environ. Microbiol.* **1999**, *65*, 1652-1657.
57. Henry, S.; Bru, D.; Stres, B.; Hallet, S.; Philippot, L. Quantitative detection of the *nosZ* gene, encoding nitrous oxide reductase, and comparison of the abundances of 16S rRNA, *narG*, *nirK*, and *nosZ* genes in soils. *Appl. Environ. Microbiol.* **2006**, *72*, 5181-5189.
58. Jones, C.M.; Graf, D.R.H.; Bru, D.; Philippot, L.; Hallin, S. The unaccounted yet abundant nitrous oxide-reducing microbial community: a potential nitrous oxide sink. *ISME J.* **2013**, *7*, 417-426.